

## Evolution of the Superconducting State of Fe-Based Compounds with Doping

S. Maiti,<sup>1</sup> M. M. Korshunov,<sup>2,3</sup> T. A. Maier,<sup>4</sup> P. J. Hirschfeld,<sup>2</sup> and A. V. Chubukov<sup>1</sup>

<sup>1</sup>*Department of Physics, University of Wisconsin, Madison, Wisconsin 53706, USA*

<sup>2</sup>*Department of Physics, University of Florida, Gainesville, Florida 32611, USA*

<sup>3</sup>*L. V. Kirensky Institute of Physics, Siberian Branch of Russian Academy of Sciences, 660036 Krasnoyarsk, Russia*

<sup>4</sup>*Computer Science and Mathematics Division and Center for Nanophase Materials Sciences, Oak Ridge National Lab, Oak Ridge, Tennessee 37831, USA*

(Received 10 April 2011; published 27 September 2011)

We introduce an effective low-energy pairing model for Fe-based superconductors with  $s$ - and  $d$ -wave interaction components and a small number of input parameters and use it to study the doping evolution of the symmetry and the structure of the superconducting gap. We argue that the model describes the entire variety of pairing states found so far in the Fe-based superconductors and allows one to understand the mechanism of the attraction in  $s^\pm$  and  $d_{x^2-y^2}$  channels, the competition between  $s$ - and  $d$ -wave solutions, and the origin of superconductivity in heavily doped systems, when only electron or only hole pockets are present.

DOI: 10.1103/PhysRevLett.107.147002

PACS numbers: 74.20.Rp, 74.62.Dh

*Introduction.*—The symmetry and structure of the superconducting gap in Fe-based superconductors (FeSCs) is the most fundamental, yet unresolved, issue in the rapidly developing field of unconventional multiband superconductivity. Although the majority of experimental and theoretical studies indicate that superconductivity in FeSCs is of electronic origin, this does not uniquely specify the gap symmetry and structure because of multiple Fermi surface (FS) sheets. These FSs appear as a result of hybridization of all five Fe  $d$  orbitals, and the interactions between low-energy fermions are a complex mixture of contributions from intra- and interorbital interactions. In this situation, an electronic mechanism of superconductivity can give rise to  $s$ -wave and non- $s$ -wave pairings, and for each symmetry the gap structure can be either conventional or extended, with  $\pi$  phase shifts between different FSs [1–3].

Previous theoretical works on FeSCs with hole and electron pockets have mostly focused on specific lattice-based models with local interactions in the orbital basis. These works have shown [2–14] that the  $s$ -wave pairing channel is generally the most attractive, although the  $d$ -wave channel is a strong competitor. An  $s$ -wave gap symmetry is consistent with angle-resolved photoemission spectroscopy data, which detected only a small variation of the gap along the hole FSs, centered at  $(0, 0)$ , and as such ruled out  $d$ -wave gap symmetry. However, for heavily hole-doped  $\text{KFe}_2\text{As}_2$  in which only hole FSs are present [15], various experimental probes [16] indicate the presence of gap nodes, which for this FS geometry are consistent with a  $d$ -wave gap.

The variety of different pairing states raised the issue of whether the physics of FeSCs is model-dependent or is universal, governed by a single underlying pairing mechanism. In this Letter, we argue that all pairing states obtained so far can be understood within the same universal

pairing scenario. We furthermore introduce the effective low-energy model with small numbers of input parameters. We conjecture that the approaches based on the RPA [2,5–8,17] renormalization-group method (both analytical [12–14] and functional [9–11,18,19]) and itinerant  $J_1 - J_2$  model [20] reduce to this model at low energies, however with different input parameters. We use this effective model to study the doping evolution of the pairing in hole- and electron-doped FeSCs. We argue that, when both hole and electron pockets are present, the pairing is driven by the pair hopping of fermions from hole to electron pockets, while at larger hole or electron doping, the pairing is due to a direct interaction between only hole or only electron pockets.

*Method.*—We treat FeSCs as itinerant systems with low-energy electronic structure consisting of hole and electron FSs. Pairing interactions between low-energy fermions  $\Gamma(\mathbf{k}_F, -\mathbf{k}_F; \mathbf{k}'_F, -\mathbf{k}'_F) \equiv \Gamma(\mathbf{k}_F, \mathbf{k}'_F)$  include intraband and interband terms and generally depend on the angles along FSs. In lattice-based models, the angle dependence is the result of dressing local interactions in the orbital basis by matrix elements associated with the hybridization of 5  $d$  orbitals. Our key assumption is that this angle dependence can be captured on general grounds, without reference to orbital models. We argue that each interaction component  $\Gamma_{ij}(\mathbf{k}_F, \mathbf{k}'_F)$  is well approximated by the leading angular harmonics in  $s$ -wave and  $d_{x^2-y^2}$ -wave channels (similar to the approximation of the  $d_{x^2-y^2}$  gap by  $\cos 2\theta$  in the cuprates). Within this leading angular harmonics approximation (LAHA),  $s$ -wave and  $d$ -wave gap equations reduce to either  $4 \times 4$  or  $5 \times 5$  sets, which can be easily solved and analyzed. This allows us to go a step further than previous works, decompose the pairing interaction into contributions from different scattering processes, and understand what causes the pairing at different dopings.

In this way we gain insight into the origin of the transition from the  $s$ -wave to the  $d$ -wave pairing and the stability of  $s$ -wave and  $d$ -wave gap structures with respect to variations of input parameters in the gap equations.

The application of LAHA to FeSCs requires some care, as electron FSs are centered at  $(0, \pi)$  and  $(\pi, 0)$  points, which are not  $k_x \leftrightarrow \pm k_y$  symmetric. As a result, some of the  $s$ -wave gap functions like  $\cos k_x + \cos k_y$  behave as  $\pm \cos 2\theta$  along the electron FSs, while some of the  $d$ -wave gap functions like  $\cos k_x - \cos k_y$  are approximated on these FSs by constants of opposite sign. With this in mind, we treated the angle-independent and  $\cos 2\phi$  terms on equal footings in both  $s$ -wave and  $d$ -wave components of the interactions. A simple analysis then shows that LAHA approximates the  $s$  and  $d_{x^2-y^2}$  components of  $\bar{\Gamma}_{ij} = N_F \Gamma_{ij}$  as

$$\begin{aligned} \bar{\Gamma}_{h_i h_j} &= u_{h_i h_j} + \tilde{u}_{h_i h_j} \cos 2\phi_i \cos 2\phi_j, \\ \bar{\Gamma}_{h_i e_1} &= u_{h_i e} (1 + 2\alpha_{h_i e} \cos 2\theta_1) \\ &\quad + \tilde{u}_{h_i e} (1 + 2\tilde{\alpha}_{h_i e} \cos 2\theta_1) \cos 2\phi_i, \\ \bar{\Gamma}_{e_1 e_1} &= u_{ee} [1 + 2\alpha_{ee} (\cos 2\theta_1 + \cos 2\theta_2) \\ &\quad + 4\beta_{ee} \cos 2\theta_1 \cos 2\theta_2] \\ &\quad + \tilde{u}_{ee} [1 + 2\tilde{\alpha}_{ee} (\cos 2\theta_1 + \cos 2\theta_2) \\ &\quad + 4\tilde{\beta}_{ee} \cos 2\theta_1 \cos 2\theta_2], \end{aligned} \quad (1)$$

where  $u_{ij}$  and  $\tilde{u}_{ij}$  are dimensionless interactions in  $s$ - and  $d$ -wave channels, respectively, and  $\phi_i$  and  $\theta_i$  label the angles along the hole and electron FSs, measured from the  $k_x$  axis. Interactions involving other electron FSs are obtained by transformations consistent with  $s$ -wave or  $d$ -wave symmetry [21].

The  $s$ -wave and  $d$ -wave gap equations within LAHA are  $4 \times 4$  matrix equations for two hole and two electron FSs and  $5 \times 5$  when the third hole FS is present. For two hole and two electron FSs the generic gap structure is

$$\begin{aligned} \Delta_{h_1}^s(\phi) &= \Delta_{h_1}^s, & \Delta_{h_2}^s(\phi) &= \Delta_{h_2}^s, \\ \Delta_{e_1}^s(\theta) &= \Delta_e^s + \bar{\Delta}_e^s \cos 2\theta, & \Delta_{e_2}^s(\theta) &= \Delta_e^s - \bar{\Delta}_e^s \cos 2\theta, \\ \Delta_{h_1}^d(\phi) &= \Delta_{h_1}^d \cos 2\phi, & \Delta_{h_2}^d(\phi) &= \Delta_{h_2}^d \cos 2\phi, \\ \Delta_{e_1}^d(\theta) &= \Delta_e^d + \bar{\Delta}_e^d \cos 2\theta, & \Delta_{e_2}^d(\theta) &= -\Delta_e^d + \bar{\Delta}_e^d \cos 2\theta, \end{aligned} \quad (2)$$

and for five FSs we add one more  $\Delta_{h_3}^{s,d}$ . We solve matrix gap equations, find the gap structure for the largest positive eigenvalue  $\lambda_{s,d}$  (if it exists), and then vary the parameters  $u_{ij}$  by hand to understand what is the mechanism for the attraction.

To verify the validity of the LAHA we compare LAHA forms of  $\Gamma(\mathbf{k}_F, \mathbf{k}'_F)$  with the full  $\Gamma(\mathbf{k}_F, \mathbf{k}'_F)$  obtained numerically in the RPA spin-fluctuation (SF) formalism starting from the 5-orbital model [6] with intra- and

interorbital hoppings and local density-density and exchange interactions  $U, V, J$ , and  $J'$ . [21] We use Eq. (1) to fit the RPA interaction  $\Gamma_{ij}$  by LAHA. In Figs. 1 and 2, we compare LAHA with the full RPA  $\Gamma_{ij}(\mathbf{k}_F, \mathbf{k}'_F)$ . The agreement is remarkably good. We analyzed eight different sets of  $U, V$ , and  $J$ , and the agreement is equally good for all sets [22]. A very few disagreements seen in the figures are cured by adding  $\cos 4\theta$  harmonics to LAHA. We verified that these extra terms do not change the gap symmetry and introduce only minor changes to the gap structure [21]. Some of the LAHA parameters extracted from the fit, which we will need for comparisons, are shown in Tables I and II. For brevity, we present only the results for dopings, when one type of pockets either almost or completely disappears. We will see that there are quite abrupt changes between the two regimes.

*Results and discussion.*—We varied the magnitudes and angle dependencies of the interactions by hand and checked what most influences the value of  $\lambda$  and the

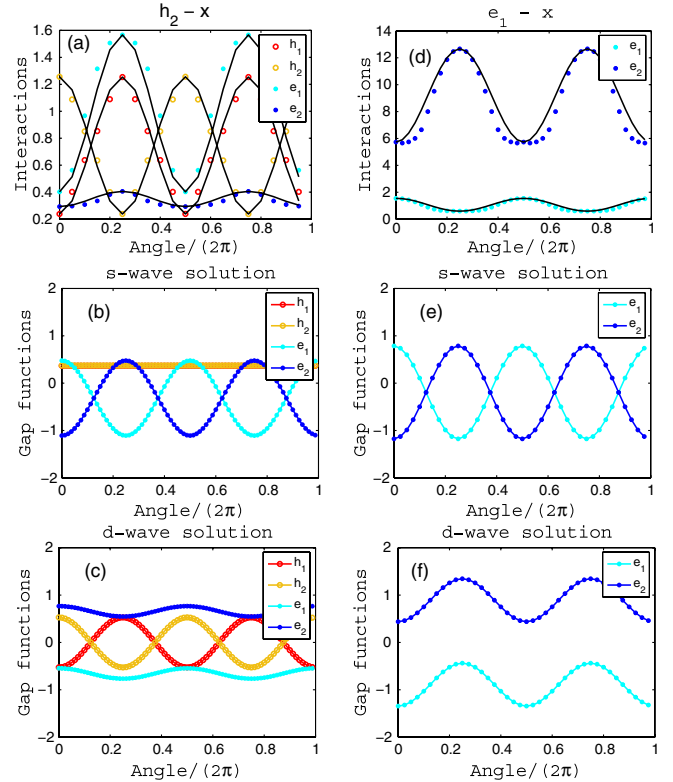


FIG. 1 (color online). Electron doping. We model electron structure by two hole FSs  $h_1$  and  $h_2$  and two electron FSs  $e_1$  and  $e_2$ . (a)–(c) Representative LAHA fit of the interactions  $\Gamma(\mathbf{k}_F, \mathbf{k}'_F)$  and resulting  $s$ - and  $d$ -wave gap functions for the case of two very tiny hole pockets.  $\mathbf{k}_F$  is taken to be along  $x$  on the  $h_2$  and  $e_1$  FSs, while  $\mathbf{k}'_F$  is varied along each of FSs. The angle is measured relative to  $k_x$ . The symbols represent the RPA interactions computed numerically; the black lines are the fits using Eq. (1). (d)–(f) are the same as (a)–(c) but for stronger electron doping, where there are no hole pockets. The parameters are presented in Ref. [22].

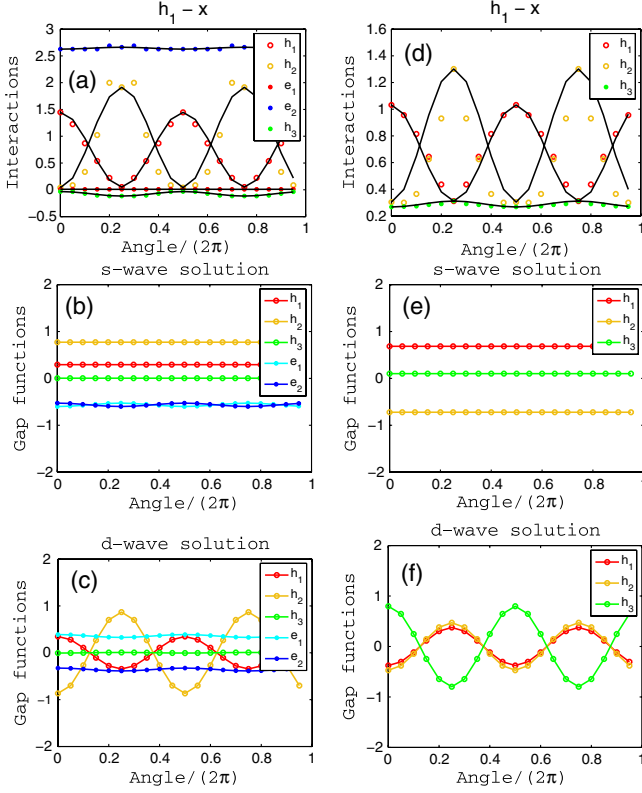


FIG. 2 (color online). The same as in Fig. 1, but for hole doping (3 hole FSs). (a)–(c) are for the case of tiny electron pockets; (d)–(f) are for stronger hole doping, when there are no electron pockets. The parameters are presented in Ref. [22].

structure of the gap. We found that some system properties are sensitive to the ratios of the parameters, but some are quite universal.

For electron doping, parameter-sensitive properties include the gap symmetry, since  $\lambda_s$  and  $\lambda_d$  remain comparable as long as both hole and electron FSs are present (see Table I), and the presence or absence of accidental nodes in the  $s$ -wave gap, although for most of the parameters the gap does have nodes, as in Fig. 1(b). The universal observation is that the driving force for attraction in both  $s$ -wave and  $d$ -wave channels is the interpocket electron-hole interaction ( $u_{h_i e}$  and  $\tilde{u}_{h_i e}$  terms), no matter how small the hole pockets are. When the SF component of the interaction is large,  $u_{h_i e}$  and  $\tilde{u}_{h_i e}$  exceed the hole-hole and electron-electron interactions. Then  $\lambda_{s,d}$  are positive already if we neglect the  $\cos 2\theta$  terms in (1) (for two equal

hole FSs the conditions are  $u_{he}^2 > u_{hh}u_{ee}$  and  $\tilde{u}_{he}^2 > \tilde{u}_{hh}\tilde{u}_{ee}$ ). In this case, the  $\cos 2\theta$  terms in the  $s$ -wave and  $d$ -wave gaps scale with the corresponding  $\alpha_{he}$ . For smaller SF component, when  $u_{he}^2 < u_{hh}u_{ee}$  (the case considered in Fig. 1 and Table I), the electron-hole interaction still generates solutions with  $\lambda_{s,d} > 0$ , only this time the gap develops a stronger  $\cos 2\theta$  component. For the input parameters that we used [22],  $u_{h_i e}$  are all positive, and the  $s$ -wave gap has a  $\pi$  shift between hole and electron FSs (an  $s^\pm$  gap). If, however,  $u_{h_i e}$  were negative, the  $s$ -wave gap would be a conventional  $s^{++}$  gap. [3]

The situation changes qualitatively once the hole pockets disappear [Figs. 1(d)–1(f)]. We see from Table I that  $\lambda_s$  is reduced, but  $\lambda_d$  is enhanced; i.e., the  $d$ -wave  $T_c$  increases. Comparing the LAHA parameters for the two dopings, we see the reason: Once the hole pockets disappear, a direct  $d$ -wave electron-electron interaction  $\tilde{u}_{ee}$  becomes attractive. To understand why this happens, we note that  $u_{ee}$  and  $\tilde{u}_{ee}$  are symmetric and antisymmetric combinations of intrapocket and interpocket electron-electron interactions:  $u_{ee} = u_{intra}^{ee} + u_{inter}^{ee}$ ,  $\tilde{u}_{ee} = u_{intra}^{ee} - u_{inter}^{ee}$ . When both  $u_{inter}^{ee}$  and  $u_{intra}^{ee}$  are positive, as in our case,  $u_{ee} > 0$ , but the sign of  $\tilde{u}_{ee}$  depends on the interplay between  $u_{inter}^{ee}$  and  $u_{intra}^{ee}$ . As long as the hole FS is present, SF are peaked near  $\mathbf{q} = (0, \pi)$  and  $(\pi, 0)$ , which are an equal distance from the relevant momenta  $\mathbf{q} = 0$  for  $u_{intra}^{ee}$  and  $\mathbf{q} = (\pi, \pi)$  for  $u_{inter}^{ee}$ . In this situation,  $u_{intra}^{ee}$  and  $u_{inter}^{ee}$  remain close in magnitude, and  $\tilde{u}_{ee}$  is small. Once the hole pocket disappears, the peak in the RPA spin susceptibility shifts towards  $(\pi, \pi)$  [17] and  $u_{inter}^{ee}$  increases more due to the SF component than  $u_{intra}^{ee}$ . A negative  $u_{inter}^{ee} - u_{intra}^{ee}$  then gives rise to a “plus-minus” gap on the two electron FSs. Such a gap changes sign between electron pockets, which differ by  $k_x \rightarrow k_y$ , and therefore has  $d_{x^2-y^2}$  symmetry [17,18]. If, however,  $u_{inter}^{ee}$  was negative and still larger by magnitude than  $u_{intra}^{ee}$ ,  $s$ -wave and  $d$ -wave couplings would interchange; i.e., the same mechanism would give rise to an  $s$ -wave pairing, with equal sign of the gaps on the two electron pockets [3]. This is the case if one uses as an input the orbital  $J_1 - J_2$  model with  $J_2 > J_1$  [20].

Next we consider the case of hole doping. The LAHA fits to the cases when electron FSs are small but still present and when only hole FSs remain are shown in Fig. 2. The parameters extracted from the fit are shown in Table II. We analyzed these and other dopings and again

TABLE I. Some of the LAHA parameters extracted from the fit in Fig. 1 for electron doping.

	Figures 1(a)–1(c)					Figures 1(d)–1(f)				
$s$ -wave	$u_{h_1 h_1}$	$u_{h_1 e}$	$\alpha_{h_1 e}$	$u_{ee}$	$\alpha_{ee}$	$\lambda_s$	$u_{ee}$	$\alpha_{ee}$	$\lambda_s$	
	0.75	0.67	-0.19	0.88	0.1	0.21	3.65	0.2	0.1	
$d$ -wave	$\tilde{u}_{h_1 h_1}$	$\tilde{u}_{h_1 e}$	$\tilde{\alpha}_{h_1 e}$	$\tilde{u}_{ee}$	$\tilde{\alpha}_{ee}$	$\lambda_d$	$\tilde{u}_{ee}$	$\tilde{\alpha}_{ee}$	$\lambda_d$	
	0.51	-0.32	-0.50	-0.05	0.9	0.35	-2.57	0.29	5.9	

TABLE II. Some of the LAHA parameters extracted from the fit in Fig. 2 for hole doping.

	Figures 2(a)–2(c)					Figures 2(d)–2(f)				
$s$	$u_{h_1 h_1}$	$u_{h_1 e}$	$\alpha_{h_1 e}$	$u_{ee}$	$\lambda_s$	$u_{h_1 h_1}$	$u_{h_1 h_2}$	$u_{h_1 h_3}$	$u_{h_3 h_3}$	$\lambda_s$
	0.75	1.36	0.08	1.40	1.8	0.67	0.8	0.29	1.37	0.13
$d$	$\tilde{u}_{h_1 h_1}$	$\tilde{u}_{h_1 e}$	$\tilde{\alpha}_{h_1 e}$	$\tilde{u}_{ee}$	$\lambda_d$	$\tilde{u}_{h_1 h_1}$	$\tilde{u}_{h_1 h_2}$	$\tilde{u}_{h_1 h_3}$	$\tilde{u}_{h_3 h_3}$	$\lambda_d$
	0.70	-1.32	0.0	1.45	1.2	0.36	-0.5	-0.02	-0.17	0.11



found universal and parameter-sensitive features. The parameter-sensitive property is again the presence or absence of accidental nodes in the  $s$ -wave gap along the electron FSs. For most of the parameters, the gap does not have nodes [see Fig. 2(b)] because  $u_{he}$  increases once it acquires an additional contribution  $u_{h_3e}$ , but for some parameters we still found nodes along the electron FSs. The universal observations are that, as long as both hole and electron pockets are present, (i) the  $s$ -wave is the leading instability ( $\lambda_s > \lambda_d > 0$ ), and (ii) the driving force for the attraction in both  $s$  and  $d$  channels is again the interpocket electron-hole interaction ( $u_{he}$  and  $\tilde{u}_{he}$  terms), no matter how small the electron pockets are. In the  $d$ -wave channel, the electron-hole interaction changes sign between the two hole FSs at (0,0); as a result,  $d$ -wave gaps on these FSs have a  $\pi$ -phase shift [see Fig. 2(c)].

The situation rapidly changes once electron pockets disappear. The  $d$ -wave eigenvalue  $\lambda_d$  grows relative to  $\lambda_s$  and for the doping shown in Fig. 2 almost exceeds it. It is very likely that the  $d$  wave becomes the leading instability at even higher dopings, and we therefore focus on the  $d$ -wave channel. Comparing  $\tilde{u}$  in Table II for the cases with and without electron pockets, we find that the  $d$ -wave channel is attractive in the absence of the electron-hole interaction because of two reasons. First, the  $d$ -wave intrapocket interaction  $\tilde{u}_{h_3h_3}$  becomes negative (attractive). Second, the interpocket interaction  $\tilde{u}_{h_1h_2}$  is larger in magnitude than the repulsive interactions  $\tilde{u}_{h_1h_1}$  and  $\tilde{u}_{h_2h_2}$ . The solutions with positive  $\lambda_d$  then exist separately for FSs  $h_{1,2}$  and  $h_3$ , and the residual interpocket interaction just sets the relative magnitudes and phases between the gaps at  $h_3$  and  $h_{1,2}$ . Because  $\tilde{u}_{h_1h_2}$  is attractive, the two  $d$ -wave gaps at  $h_{1,2}$  are now in phase; i.e., this  $d$ -wave solution is a different eigenfunction from the one with phase shift  $\pi$  at smaller dopings. The difference is clearly seen by comparing Figs. 2(c) and 2(f). The  $d$ -wave gap symmetry at large doping and in-phase structure of the gaps at  $h_{1,2}$  is consistent with the functional renormalization-group solution [19]. Note, however, that the  $s$ -wave channel is also attractive. The  $s$ -wave gap changes sign between the two FSs at (0,0) and is small on the  $(\pi, \pi)$  FS.

**Conclusions.**—In this work, we derived and analyzed the effective low-energy model for FeSCs with a minimal number of parameters. We argued that the model captures the key physics of the pairing at all dopings. We found that the same pairing mechanism—spin-fluctuation exchange—determines the pairing for all dopings, but the specifics of the pairing and the symmetry and structure of the pairing gap is different in FeSCs with hole and electron FSs from the ones at strong hole or electron doping, when only one type of FS remains. At small to moderate dopings, the pairing is  $s$ -wave, driven by interpocket electron-hole interaction, no matter how small hole or electron FSs are. At strong electron doping, the pairing is  $d$ -wave, driven by

$d$ -wave attraction between the electron pockets, and at strong hole doping the pairing is either  $d$ -wave, driven by  $d$ -wave attraction within one of hole pockets, or  $s$ -wave, driven by the interaction between hole pockets at (0,0). It would be extremely interesting to understand whether the pairing symmetry and the structure of gaps along hole FSs change in  $\text{Ba}_{1-x}\text{K}_x\text{Fe}_2\text{As}_2$  with increasing  $x$ . Whether the  $\text{KFe}_2\text{Se}_2$ -type materials, which have only electron FSs [23,24], are  $d$ -wave superconductors remains to be seen.

We acknowledge helpful discussions with L. Benfatto, A. Bernevig, R. Fernandes, W. Hanke, I. Eremin, Y. Matsuda, I. Mazin, R. Prozorov, D. Scalapino, Z. Tesanovic, R. Thomale, M. Vavilov, and A. Vorontsov. This work was supported by NSF-DMR-0906953 (S.M. and A.V.C.), DOE DE-FG02-05ER46236 (P.J.H.), the Center for Nanophase Materials Sciences, sponsored at ORNL by the Office of Basic Energy Sciences, DOE (T.A.M.), and RFBR 09-02-00127, Presidium of RAS program N5.7, FCP GK P891, and President of Russia MK-1683.2010.2 (M.M.K.). We are grateful to KITP at Santa Barbara for its hospitality during the work on this manuscript.

- 
- [1] See, e.g., H.H. Wen and S. Li, *Annu. Rev. Condens. Matter Phys.* **2**, 121 (2011); P.J. Hirschfeld, M.M. Korshunov, and I.I. Mazin, arXiv:1106.3712.
  - [2] T.A. Maier *et al.*, *Phys. Rev. B* **79**, 224510 (2009).
  - [3] H. Kontani and S. Onari, *Phys. Rev. Lett.* **104**, 157001 (2010); T. Saito, S. Onari, and H. Kontani, *Phys. Rev. B* **83**, 140512(R) (2011).
  - [4] K. Kuroki *et al.*, *Phys. Rev. B* **79**, 224511 (2009).
  - [5] H. Ikeda, R. Arita, and J. Kunes, *Phys. Rev. B* **81**, 054502 (2010).
  - [6] S. Graser, T.A. Maier, P.J. Hirschfeld, and D.J. Scalapino, *New J. Phys.* **11**, 025016 (2009); see also C. Cao, P.J. Hirschfeld, and H.-P. Cheng, *Phys. Rev. B* **77**, 220506(R) (2008).
  - [7] A.F. Kemper *et al.*, *New J. Phys.* **12**, 073030 (2010).
  - [8] S. Graser *et al.*, *Phys. Rev. B* **81**, 214503 (2010).
  - [9] C. Platt, C. Honerkamp, and W. Hanke, *New J. Phys.* **11**, 055058 (2009); R. Thomale *et al.*, *Phys. Rev. B* **80**, 180505 (2009).
  - [10] R. Thomale *et al.*, *Phys. Rev. Lett.* **106**, 187003 (2011).
  - [11] F. Wang, H. Zhai, and D.-H. Lee, *Phys. Rev. B* **81**, 184512 (2010).
  - [12] V. Cvetkovic and Z. Tesanovic, *Phys. Rev. B* **80**, 024512 (2009).
  - [13] A.V. Chubukov, D.V. Efremov, and I. Eremin, *Phys. Rev. B* **78**, 134512(R) (2008).
  - [14] S. Maiti and A.V. Chubukov, *Phys. Rev. B* **82**, 214515 (2010).
  - [15] T. Sato *et al.*, *Phys. Rev. Lett.* **103**, 047002 (2009); T. Terashima *et al.*, *J. Phys. Soc. Jpn.* **79**, 053702 (2010).
  - [16] J.K. Dong *et al.*, *Phys. Rev. Lett.* **104**, 087005 (2010); K. Hashimoto *et al.*, *Phys. Rev. B* **82**, 014526 (2010).
  - [17] T.A. Maier *et al.*, *Phys. Rev. B* **83**, 100515(R) (2011).
  - [18] F. Wang *et al.*, *Europhys. Lett.* **93**, 57003 (2011).

- [19] R. Thomale *et al.*, *Phys. Rev. Lett.* **107**, 117001 (2011).
- [20] R. Yu *et al.*, [arXiv:1103.3259](https://arxiv.org/abs/1103.3259); C. Fang *et al.*, [arXiv:1105.1135](https://arxiv.org/abs/1105.1135) [*Phys. Rev. X* (to be published)].
- [21] See Supplemental Material at <http://link.aps.org/supplemental/10.1103/PhysRevLett.107.147002> for details of the RPA formalism, LAHA formalism, derivation of the matrix gap equations, and checks with higher harmonics.
- [22] We used the same 2D band structure parameters as in Ref. [6] and set  $\mu = \pm 0.18$  ( $n_e = 6.22$  and  $n_e = 5.53$ ) for the cases of tiny electron or hole FSs and  $\mu = \pm 0.3$  ( $n_e = 6.31$  and  $n_e = 4.88$ ) for the cases when no hole or electron FSs remain (all parameters are in eV). We did computations for  $\mu = \pm 0.05$  and  $\mu = \pm 0.1$  and obtained similar results as for  $\mu = \pm 0.18$ . For electron doping we used 6 different set of parameters and got similar results for all sets. The ones we used in Figs. 1 and 2 are  $U = 1$ ,  $J = 0.25$ , and  $V = 0.69$ . For hole doping, we used  $U = 0.9$ ,  $J = 0$ , and  $V = 0.9$  for  $\mu = -0.18$  and  $U = 0.75$ ,  $J = 0.15$ , and  $V = 0.46$  for  $\mu = -0.3$  to avoid spin ordering instability. For  $\mu = -0.3$ , we show the results for the band structure from Ref. [17]. The results for the band structure from Ref. [6] are qualitatively the same, but  $\tilde{u}_{ee}$  and  $\lambda_d$  are smaller.
- [23] J.-G. Guo *et al.*, *Phys. Rev. B* **82**, 180520(R) (2010).
- [24] T. Qian *et al.*, *Phys. Rev. Lett.* **106**, 187001 (2011).